Peer-reviewed version available at *Minerals* **2019**, *9*, 490; doi:10.3390/min9080490

Article

Pyrochlore-Group Minerals in the Granite-Hosted Katugin Rare-Metal Deposit, Transbaikalia, Russia

Anastasia E. Starikova [1,2,*], Ekaterina P. Bazarova [3], Valentina B. Savelieva [3], Eugene V. Sklyarov [3,4], Elena A. Khromova [5] and Sergei V. Kanakin [5]

[1] V.S. Sobolev Institute of Geology and Mineralogy, Siberian Branch of the Russian Academy of Sciences, 3 Akad. Koptyug av., Novosibirsk 630090, Russia; starikova@igm.nsc.ru
[2] Novosibirsk State University, 2 Pirogov st., Novosibirsk, 630090, Russia; starikova@igm.nsc.ru
[3] Institute of the Earth's Crust, Siberian Branch of the Russian Academy of Sciences, 128 Lermontova st., Irkutsk 664033, Russia; bazarova@crust.irk.ru (E.P.B.); vsavel@crust.irk.ru (V.B.S.); skl@crust.irk.ru (E.V.S.)
[4] Far East Federal University, 8 Sukhanov st., Vladivostok 690091, Russia; skl@crust.irk.ru
[5] Geological Institute, Siberian Branch of the Russian Academy of Sciences, 6a, Sakhjanova st., lena.khromova@mail.ru (E.A.S); skan_61@mail.ru (S.V.K.)
* Correspondence: starikova@igm.nsc.ru; Tel.: +7-913-207-8362 (A.E.S.)

Received: date; Accepted: date; Published: date

Abstract: Pyrochlore group minerals are the main raw phases in granitic rocks of the Katugin complex-ore deposit that stores Nb, Ta, Y, REE, U, Th, Zr, and cryolite. They are of three main generations: primary magmatic (I), early postmagmatic (II), and supergene (III) pyrochlores. The primary magmatic phase (generation I) is fluornatropyrochlore with high concentrations of Na_2O (to 10.5 wt.%), F (to 5.4 wt.%) and REE_2O_3 (to 17.1 wt.%) but low CaO (0.6-4.3 wt.%), UO_2 (to 2.6 wt.%), ThO_2 (to 1.8 wt.%), and PbO (to 1.4 wt.%). Pyrochlore of this type is very rare in nature and limited to a few occurrences, such as rare-metal deposits of Nechalacho in syenite and nepheline syenite (Canada) and Mariupol in nepheline syenite (Ukraine). It may have crystallized synchronously with or slightly later than melanocratic minerals (aegirine, biotite, and arfvedsonite) at the late magmatic stage when Fe from the melt became bound making impossible the formation of columbite. Second generation pyrochlore formed at the early postmagmatic stage of the Katugin deposit. It differs from that of first generation in lower Na_2O concentrations (2.8 wt.%), relatively low F (4 wt.%), and les occupancy of the A and Y sites at similar contents of other components. Generation III pyrochlore is a product of supergene alteration processes. It is compositionally heterogeneous and contains K, Ba, Pb, Fe, and significant Si concentrations but low Na and F. Its compositions mostly fall within the filed of hydro- and kenopyrochlore.

Keywords: pyrochlore-group minerals, fluornatropyrochlore, alkaline granites, Katugin rare-metal deposit, East Transbaikalia

1. Introduction

Pyrochlore-group minerals are broadly occurring in nature and are of important economic interest due to their ability to host Ta, Nb, U, and REE. They are common accessory phases in carbonatite and are often found in such lithologies as nepheline syenite, alkaline gabbro and granitoids, pegmatite, and in albite and greysen granites [1-6, etc.]. Pyrochlore minerals have diverse compositions with the general formula $A_{2-m}B_2O_{6-w}Y_{1-n}$, where A represents large cations (Na, Ca, U, Th, REE, Y, Sr, Ba, Pb, Sn, and H_2O) and site vacancies, the B-site is occupied by smaller cations (Nb, Ti, and Ta), and Y is occupied by F, OH^-, O^{2-} and H_2O or site vacancies [7-9]. The symbols *m*, *w*, and *n* represent parameters indicating incomplete occupancy of the *A*, *X*, and *Y*.

Preprints (www.preprints.org) | NOT PEER-REVIEWED | Posted: 30 June 2019

Peer-reviewed version available at *Minerals* **2019**, *9*, 490; doi:10.3390/min9080490

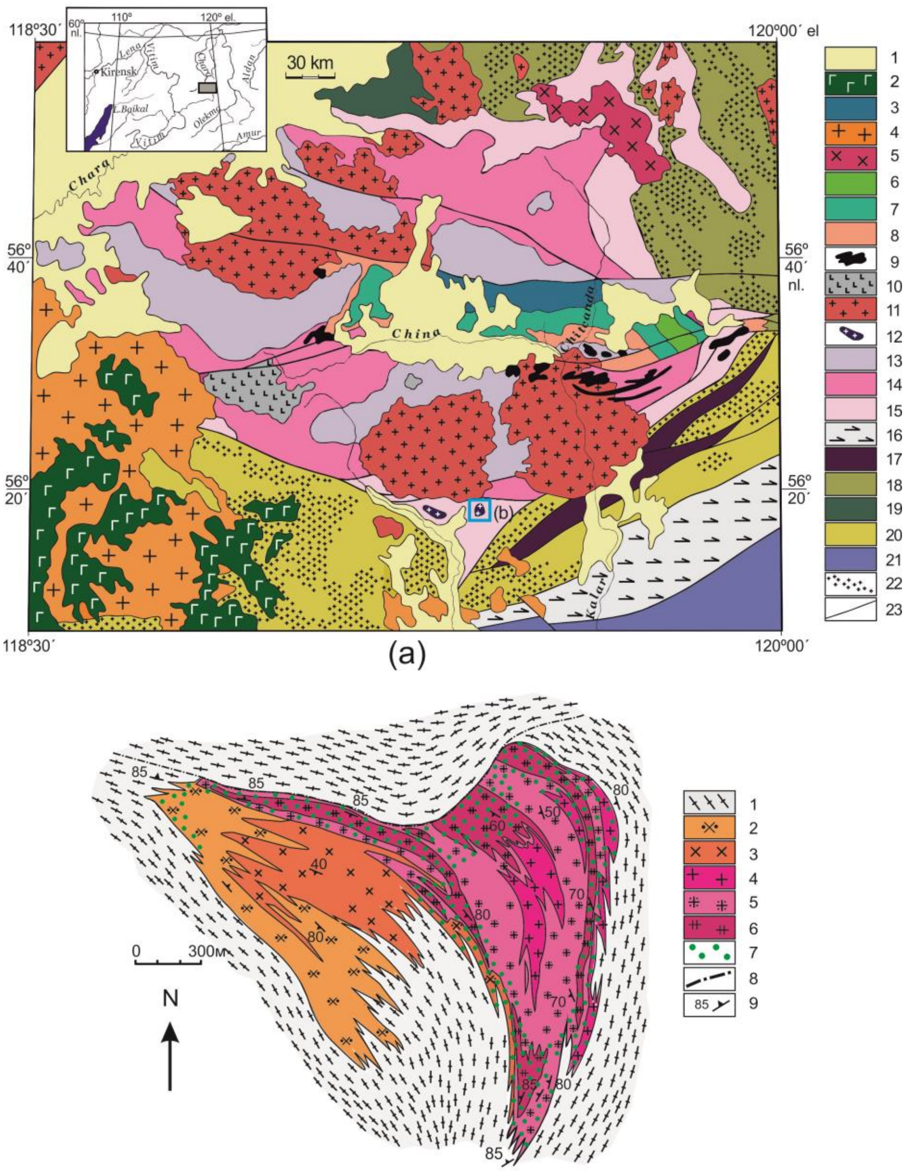

(b)

Figure 1. a: Simplified geological map of the region of the Katugin granite complex, after [11,12]. 1 = Quaternary sediments; 2 = flood basalts (N_2-Q); 3 = Jurassic coal-bearing clastic sediments; 4 = granite, granodiorite, granosyenite and monzonite of the Ingamakit complex (PZ_3); 5 = nepheline syenite, granosyenite and monzonite of the Khanin complex (PZ_3); 6 = Ordovician variegated sediments; 7 = Cambrian variegated sediments; 8 = Vendian variegated sediments; 9 = gabbro-dolerite, gabbro and dolerite porphyrite of the Doros complex; 10 = layered plutons of the Chinei complex; 11 = granite of the Kodar complex; 12 = rare-metal granite of the Katugin complex; 13-15 = carbonate and clastic sediments of the Udokan supergroup: Kemen group (13), Chinei group (14), Kodar group (15); 16 = anorthosite of the Kalar complex; 17 = low-grade metamorphic volcanic-sedimentary rocks of the Subgan complex; 18 = tonalite-trondjemite orthogneis of the Olekma complex; 19 = Chara sequence (garnet-biotite and garnet-hypersthene-biotite plagiogneiss, mafic schists, quartzite and magnetite quartzite); 20 = Kalar sequence (garnet-biotite plagiogneiss with layers and lenses of two-pyroxene mafic granulite, clac-silicate rocks, quartzite, and magnetite quartzite; 21 = metamorphic and igneous complexes of the Selenga-Stanovik superterrane in the Central Asian orogenic belt; 22 = zones of widespread Precambrian granitic rocks; 23 = faults.
b: Simplified geology of the Katugin granite intrusion, after [13,14]. 1 = gneiss, migmatite, blastomylonite of the Kodar group, Udokan group; 2-6 = Katugin granites of different types: biotite (2), biotite-riebeckite (3), biotite-arfvedsonite (4), arfvedsonite (5), aegirine-arfvedsonite and aegirine (6); 7 = ore-bearing granite; 8 = faults; 9 = bedding elements.

Peer-reviewed version available at *Minerals* **2019**, *9*, 490; doi:10.3390/min9080490

The Ca/Na ratios vary considerably. Fluorcalciopyrochlore $(Ca,Na)_2Ca_2O_6F$ is the most widespread phase in the group [3,8,10]. Findings of pyrochlore with prominent Na enrichment over Ca and other cations at the A-site are very few and limited to several rare-metal deposits hosted by the Nechalacho syenite and nepheline syenite (Canada) [15,16], the Mariupol nepheline syenite (Ukraine) [17], the Strange Lake granite (Canada) [18], and the Halzdan-Buregteg alkaline granite (West Mongolia) [19]. Fluornatropyrochlore $(Na,Pb,Ca,REE,U)_2Nb_2O_6F$ was reported as a mineral species from the Boziguoer granites (China) only in 2013 [20].

This paper focuses on high-Na pyrochlores from the Katugin rare-metal deposit hosted by alkaline granites. In previous publications, pyrochlores were described in brief among other rock-forming, ore and accessory minerals [13,21,22], mostly based on monofraction wet chemistry data and few EPMA determinations.

2. Geological setting

The Katugin deposit extremely rich in REE, Nb, and Ta is located in the Aldan shield, at the southern margin of the Chara-Olekma terrane near the border with terranes of the Central Asian Orogenic Belt marked by the Stanovik suture [23]. The ores are hosted by two relatively small (3 and 18 km^2) A-type alkaline granite intrusions of the Katugin complex [11,13] (Fig.1a), which were earlier interpreted as alkaline metasomatites [21,, 24-26]. The Western intrusion is 80% buried under a moraine and remains quite poorly documented. The heart-shaped Eastern intrusion (Fig. 1b) is composed of three types of granites corresponding to three phases of magmatism [11,13]: phases I, II, and III, respectively, of biotite (Bt) and biotite-riebeckite (Bt-Rbk), biotite-arfvedsonite (Bt-Arf), and arfvedsonite, aegirine-arfvedsonite and aegirine (Arf, Aeg-Arf, Aeg) granites. Phase III granites have diverse mineralogy and lack distinct boundaries. They are joined into one phase because the Aeg, Aeg-Arf, and Arf varieties may grade from one to another in a single sample. All types are medium- and fine-grained, often gneissic, leucocratic and mesocratic quartz-albite-microcline granites with variable amounts of melanocratic minerals; some arfvedsonite and aegirine granites appear as isolated pegmatitic veins.

Biotite and biotite-riebeckite granites (phase I) have moderate or high Al contents and quite high CaO, but contain the smallest amount of F among all granites we sampled. Biotite-arfvedsonite granites (phase II) are supersaturated with respect to alkalis, rich in CaO and Y, but poor in Na_2O and F. The ore-bearing granites of phase III are likewise supersaturated in alkalis; they have high concentrations of Na_2O and F but very low CaO, and are mostly rich in Zr, Hf, Nb, and Ta [11].

The Katugin granites host Zr, Ta-Nb-REE, and F-Al mineralization [21,22]. Zircons are present either as sporadic grains or as large clusters (to 20 vol.%) in all rocks of the intrusion. Fluoraluminate minerals include abundant cryolite (a large body on the intrusion margin and ≤3 cm globules in Aeg granites) and smaller percentages of other phases (weberite, chiolite, prosopite, pachnolite, thomsenolite, and Ba-fluoraluminates). Ta-Nb-REE phases are mainly pyrochlore, columbite-(Fe), monazite-(Ce), fluorides (fluorzerite-(Ce), gagarinite-(Y), tveitite-(Y), yttrofluorite) and fluorcarbonates (bastnäsite-(Ce) and parizite-(Ce)) or less often monazite-(Ce). REE fluorides and fluorcarbonates often form aggregates unevenly distributed in the rocks [27,28]. Other minerals are ilmenite, magnetite, and sulfides (sphalerite, galena, pyrrhotite or pyrite). The mineralization is roughly coeval to the host intrusion (2055±7 Ma against 2066±6 Ma) [23,29].

3. Materials and Methods

The analytical work was performed at the Analytical Center for Multielement and Isotope Studies of the V.S. Sobolev Institute of Geology and Mineralogy (Novosibirsk, Russia) and at the Analytical Center for Mineralogical, Geochemical, and Isotope Studies of the Geological Institute (Ulan-Ude, Russia). We analyzed pyrochlore monofractions from different types of the Katugin granites: biotite, biotite-riebeckite, biotite-arfvedsonite, arfvedsonite, aegirine-arfvedsonite, and aegirine granites, as well as aegirine granite enriched in zircon, pyrochlore, and REE phases (the ore-rich aegirine granite). The mineral phases were identified and analyzed using a *Carl Zeiss LEO-1430VP* scanning electron microscope equipped with an Oxford Instruments *INCAEnergy 350*

Peer-reviewed version available at *Minerals* **2019**, *9*, 490; doi:10.3390/min9080490

energy-dispersive microanalysis system (EDS method, Analysts E.A. Khromova and S.V. Kanakin, Geological Institute, Ulan-Ude). The electron beam was operated at an accelerating voltage of 20 kV, a beam current of >0.5 nA, X-ray generation region of 2-3 µm, and a count time of 50 s. Most of analyses were applied to small zones of preparations in order to reduce the effect of grain surface microtopography. Some phases were identified using point by point analyses when necessary. Element concentrations in pyrochlores were measured on a Jeol *JXA-8100* electron-microprobe analyzer (WDS method) at the Institute of Geology and Mineralogy, Novosibirsk (analyst E.N. Nigmatulina). The operation conditions were: 2 µm beam diameter, 30 nA beam current, 20 kV accelerating voltage, and 10 s count time on peak per element. The results were calibrated using the following standards: albite (Na, Al, Si); diopside (Ca); F-phlogopite (F, K, and Mg); $LiNbO_3$ (Nb); rutile (Ti); Ta_2O_5 (Ta); zircon (Zr); UO_2 (U); ThO_2 (Th); SrSi glass (Sr); PbTe (Pb); BaSi glass (Ba); $KLaMoO_4$ (La); $LiCeWO_4$ (Ce); $CsPrMoO_4$ (Pr); $RbNdWO_4$ (Nd); $LiSmMoO_4$ (Sm); $LiGdMoO_4$ (Gd); $LiDyWO_4$ (Dy); and $Y_3Al_5O_{12}$ (Y). The PAP program was applied for matrix correction. The error was less than 2 rel.% for major elements.

4. Results

Pyrochlore-group minerals are main ore phases of the Katugin rare-metal deposit common to different granitic rocks of the complex, except for Bt and Bt-Rbk granites of phase I which bear columbite-(Fe) as a predominant opaque mineral while pyrochlores are few. Pyrochlore is especially abundant in phase III Aeg and Aeg-Arf granites where it occurs as round or rarely octahedral euhedral grains (≤5 mm) or as clusters and lenses, including in ore-rich zones. The pyrochlore grains are honey-yellow to almost black but most often brown, with signatures of replacement by later generations (Fig. 2). There are three main generations of pyrochlore identified according to crystallization sequence and chemistry. Early (I generation) pyrochlores are isolated crystals or aggregates. Second-generation pyrochlores, looking darker-shaded in BSE images, follow cracks or replace earlier pyrochlore in grain rims (Fig. 2); some occur in crystalline inclusions in zircon from

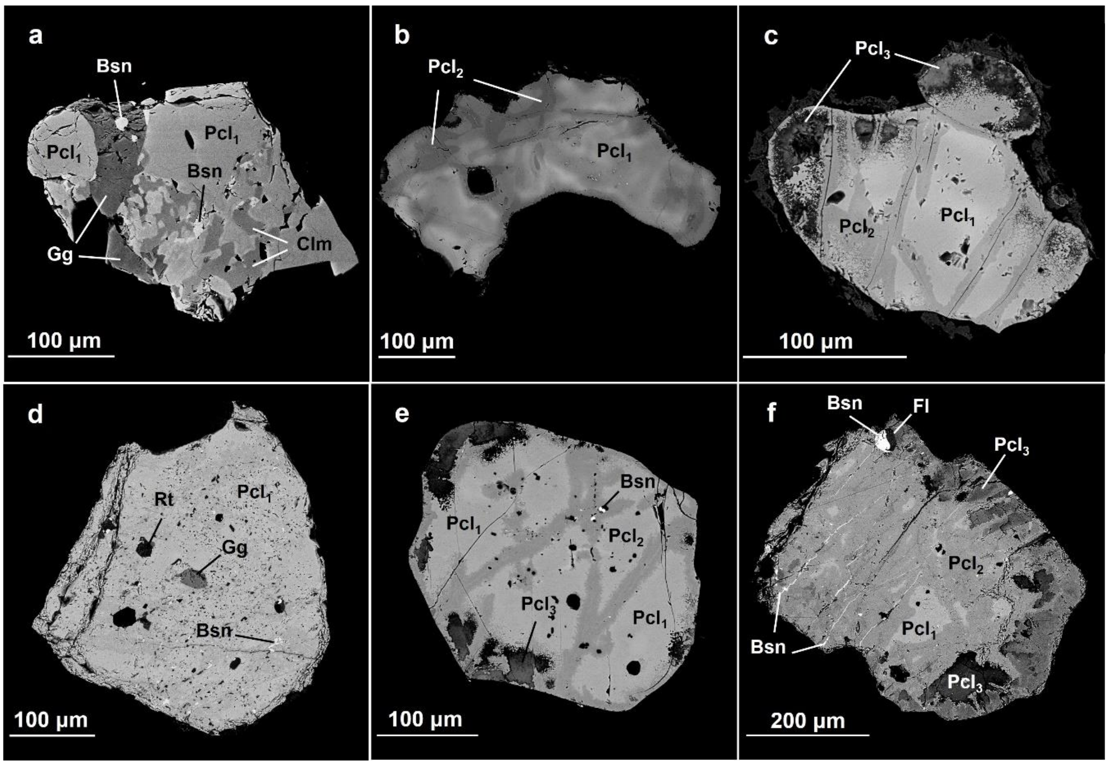

Figure 2. Pyrochlore-group minerals from the Katugin granites of different types (BSE image). a, b: Bt-Arf granite; c: Bt-Rbk granite; d: Aeg-Arf granite; e, f: Aeg granite. Mineral names are abbreviated as Bsn = bastnäsite, Clm = columbite, Fl = fluorite, Gg = gagarinite-(Y), Pcl_1 = first-generation pyrochlore, Pcl_2 = second-generation pyrochlore, Pcl_3 = third-generation pyrochlore, Rt = rutile.

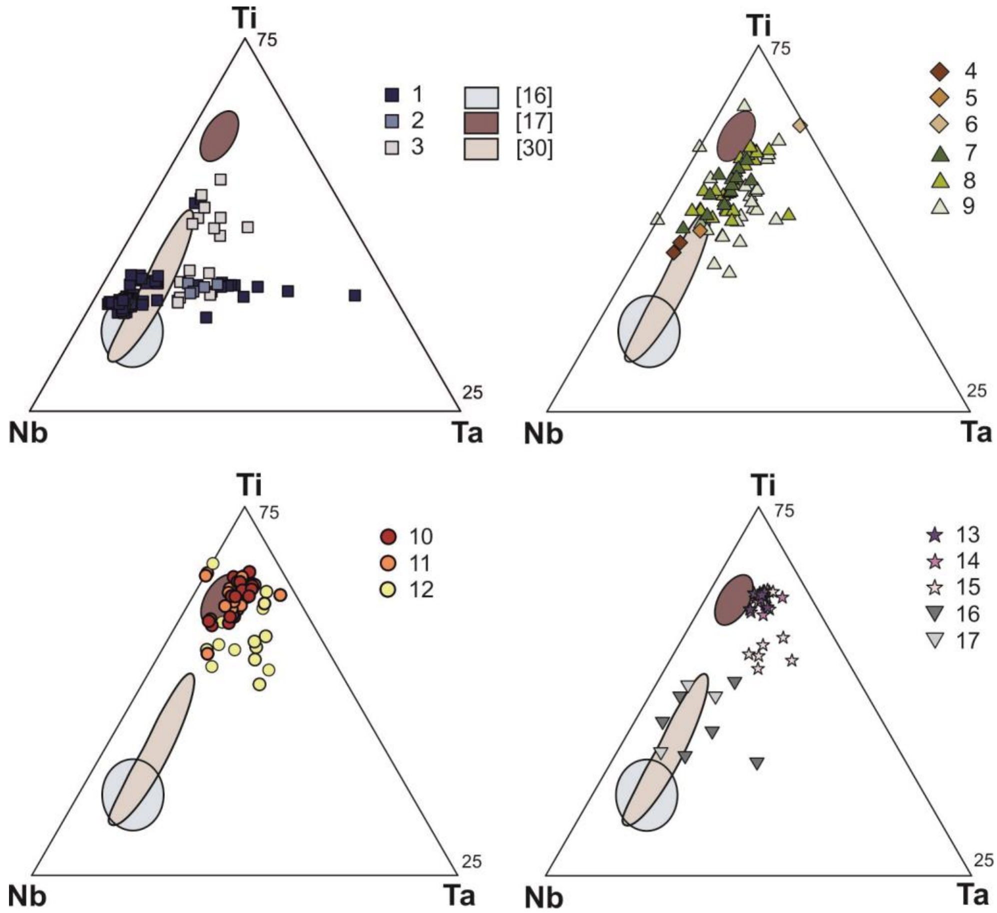

Figure 3. Ternary classification diagrams (B-site) for pyrochlore-group minerals from the Katugin granites: 1-3 = first- (1), second- (2), and third- (3) generation pyrochlores from Bt-Arf granite; 4-6 = first- (4), second- (5), and third- (6) generation pyrochlores from Arf granite; 7-9 = first- (7), second- (8), and third- (9) generation pyrochlores from Arf-Aeg granite; 10-12 = first- (10), second- (11), and third- (12) generation pyrochlores from Aeg granite; 13-15 = first- (13), second- (14), and third- (15) generation pyrochlores from ore-rich Aeg granite; 16-17 = first- (16) and second- (17) generation pyrochlores from Bt granite. [16], [17], [30] = fields of fluornatropyrochlores from literature [16,17,30], respectively.

Aeg-Arf granites. Late (III generation) pyrochlore appears in most strongly altered and deformed grain parts. In Bt-Arf granites, early pyrochlore is rarely replaced by later phases but rather by aggregates of columbite, gagarinite-(Y), and bastnäsite-(Ce) (Fig. 2 a). Pyrochlore from Aeg, Aeg-Arf, and Arf granites (phase III) often encloses numerous veinlets or microcrystals (10 μm on average) of other phases (bastnäsite-(Ce), gagarinite-(Y), yttrofluorite, and occasionally rutile) produced by alteration (Fig.2 f). Columbite-(Fe) replaces pyrochlore in some grains. Some pyrochlores enclose cryolite, quartz, albite, feldspar, aegirine, zircon, and magnetite.

4.1. First-generation pyrochlore

Among early pyrochlores, the (#Nb) pyrochlore-group end-members predominates over those of microlite (#Ta) or betafite (#Ti) groups in all analyses (Fig. 3; Tables 1-3). The B-site is occupied by 73-90 at.% of Nb, 7.5-23 at.% of Ti, and 0-15 at.% of Ta. The B-site is occupied by 73-90 at.% of Nb, 7.5-23 at.% of Ti, and 0-15 at.% of Ta. The A-site accommodates large cations of Na, REE+Y, and Ca (Fig. 4), as well as U, Th and Pb (no more than 6 at.% in total); other cations occur in minor amounts. REE are mainly Ce while HREE and Y are low. Abundant F occupies the Y-site (Fig. 5).

First-generation pyrochlore from Bt-Arf granites differs from those in other granite types and contains as much as 6.4 to 10.7 wt.% Na_2O (Fig.5; Table 1), which exceeds previously reported values from different occurrences worldwide (within 9.18 wt.% Na_2O) [12]. It is also rich in niobium (up to

Preprints (www.preprints.org) | NOT PEER-REVIEWED | Posted: 30 June 2019

Peer-reviewed version available at *Minerals* **2019**, *9*, 490; doi:10.3390/min9080490

Table 1. Chemistry (wt.%) of pyrochlore-group minerals from the Katugin biotite-arfvedsonite granite (WDS analyses).

	I						II		III		
	1	2	3	4	5	6	n=12	sd	n=8	min	max
SiO_2	bd	bd	bd	bd	bd	bd	0.02	0.06	4.47	1.49	7.40
TiO_2	2.84	2.79	3.05	2.67	2.85	3.05	4.20	1.19	3.66	2.64	4.56
Al_2O_3	bd	bd	bd	bd	bd	bd	bd	-	0.17	bd	0.30
CaO	1.68	1.66	3.23	3.47	2.78	3.19	3.53	1.26	2.44	0.19	3.52
Na_2O	10.46	9.18	8.60	9.95	7.22	6.77	2.25	1.24	1.11	3.07	1.26
K_2O	bd	bd	bd	bd	bd	bd	bd	0.02	0.54	0.06	1.31
Ce_2O_3	8.3	8.72	6.15	5.97	7.81	7.92	7.45	1.23	4.36	1.84	6.55
La_2O_3	2	2.14	1.24	1.42	2.18	2.08	2.00	0.56	0.86	0.34	1.75
Pr_2O_3	1.18	1.06	0.90	0.77	0.88	0.85	0.78	0.11	0.38	bd	0.68
Nd_2O_3	3.52	3.51	3.2	2.78	2.56	2.53	2.39	0.45	1.11	0.53	1.91
Sm_2O_3	0.75	0.83	1.02	0.83	0.50	0.47	0.49	0.13	0.26	bd	0.46
Gd_2O_3	0.45	0.30	0.82	0.81	0.38	0.28	0.29	0.15	0.15	bd	0.28
Dy_2O_3	0.25	0.24	0.60	0.65	0.24	0.17	0.14	0.08	bd	bd	bd
Y_2O_3	0.49	0.53	0.90	1.29	bd	0.56	0.19	0.24	0.09	bd	0.30
ThO_2	1.30	1.51	0.84	0.69	0.81	0.82	1.35	0.69	1.26	0.73	1.63
UO_2	0.37	0.39	0.70	0.66	1.49	1.56	1.76	0.18	2.19	1.68	3.06
PbO	bd	bd	bd	bd	0.11	0.11	0.54	0.75	1.28	bd	2.31
Nb_2O_5	57.99	59.23	60.42	59.21	47.22	51.14	55.71	1.67	50.06	46.13	55.38
Ta_2O_5	2.64	2.06	2.20	2.27	15.23	11.51	4.54	1.42	5.03	4.39	6.13
SrO	bd	bd	bd	bd	bd	bd	0.09	0.17	0.96	0.28	1.55
BaO	bd	bd	bd	bd	bd	bd	0.15	0.23	1.90	bd	2.94
F	4.62	4.73	4.69	4.72	4.31	4.61	4.26	0.46	2.28	0.63	3.91
Total	98.84	98.88	98.55	98.17	96.57	97.61	92.13		84.87		
O_2=F	1.95	1.99	1.97	1.99	1.82	1.94	1.79		0.96		
Total	96.9	96.89	96.58	96.18	94.76	95.67	90.33		83.91*		
ΣREE_2O_3	16.45	16.79	13.93	13.23	14.55	14.30	13.53		7.12		
Na	1.395	1.210	1.104	1.313	1.013	0.920	0.295		0.136		
Ca	0.124	0.121	0.229	0.253	0.216	0.239	0.256		0.165		
K	-	-	-	-	-	-	-		0.044		
LREE	0.394	0.401	0.300	0.290	0.367	0.353	0.323		0.161		
HREE	0.016	0.012	0.031	0.033	0.015	0.010	0.009		0.003		
Y	0.018	0.019	0.032	0.047	-	0.021	0.007		0.003		
Th	0.020	0.023	0.013	0.011	0.013	0.013	0.021		0.018		
U	0.006	0.006	0.010	0.010	0.024	0.024	0.027		0.031		
Pb	-	-	-	-	0.002	0.002	0.010		0.022		
Sr	-	-	-	-	-	-	0.003		0.035		
Ba	-	-	-	-	-	-	0.004		0.047		
ΣA	1.973	1.792	1.718	1.956	1.650	1.583	0.954		0.62		
Al	-	-	-	-	-	-	-		0.013		
Si	-	-	-	-	-	-	0.001		0.283		
Ti	0.147	0.143	0.152	0.137	0.155	0.161	0.213		0.174		
Nb	1.804	1.819	1.809	1.821	1.545	1.620	1.702		1.433		
Ta	0.049	0.038	0.040	0.042	0.300	0.219	0.084		0.087		
ΣB	2.000	2.000	2.000	2.000	2.000	2.000	2.000		2.000		
F	1.006	1.017	0.981	1.017	0.988	1.021	0.911		0.456		
#Nb	90.18	90.97	90.43	91.07	77.26	81.00	85.15		84.61		
#Ti	7.35	7.13	7.59	6.83	7.76	8.04	10.67		10.27		
#Ta	2.47	1.90	1.98	2.10	14.99	10.97	4.178		5.12		

Note: 1-4 = pyrochlores without visible zoning; 5, 6 = rims in zoned pyrochlores. *n* is number of analyses; sd is standard deviation; numerals I, II, III correspond to pyrochlore generations, bd is below detection limit. For compositionally variable third-generation pyrochlores, minimum (min) and maximum (max) contents are given instead of standard deviations. Formula based on 2 cations at B-site. #Nb, #Ti, #Ta are pyrochlore, betafite, and microlite end-member components (mol.%), respectively. * - Sum also includes 0.07 wt.% Fe_2O_3 and 0.19 ZrO_2.

Peer-reviewed version available at *Minerals* **2019**, *9*, 490; doi:10.3390/min9080490

Table 2. Chemistry (wt.%) of pyrochlore-group minerals from the Katugin biotite and biotite-riebeckite granites (1) and arfvedsonite aegirine-arfvedsonite granites (2).

	1				2						
	I		II		I		II		III		
	n=7	sd	n=3	sd	n=11	sd	n=21	sd	n=23	min	max
SiO_2	bd	-	1.51	0.23	bd	-	0.02	0.07	5.47	2.34	9.24
TiO_2	4.33	0.87	4.3	0.97	5.92	0.91	6.27	0.82	5.04	2.81	6.54
Al_2O_3	bd	-	bd	-	bd	-	bd	-	0.23	bd	0.64
Fe_2O_3	bd	-	bd	-	bd	0.01	bd	0.01	0.17	bd	2.05
CaO	3.71	1.05	2.85	0.44	3.56	1.28	2.52	1.69	1.34	0.39	3.06
Na_2O	6.61	0.63	2.66	1.56	6.91	0.96	3.00	0.50	1.90	0.20	3.83
K_2O	bd	-	bd	-	bd	-	bd	0.02	0.45	0.15	1.17
Ce_2O_3	8.55	1.32	8.80	0.93	6.85	0.77	7.11	0.66	5.49	3.10	7.92
La_2O_3	2.19	0.35	2.15	0.45	1.44	0.64	1.43	0.33	0.78	0.26	1.59
Pr_2O_3	0.36	0.59	bd	-	0.73	0.11	0.77	0.18	0.50	0.24	0.77
Nd_2O_3	3.29	0.31	3.06	0.28	2.58	0.42	2.55	0.38	1.35	0.61	2.32
Sm_2O_3	bd	-	bd	-	0.69	0.15	0.76	0.18	0.43	0.16	0.69
Gd_2O_3	bd	-	bd	-	0.58	0.20	0.70	0.32	0.32	bd	0.66
Dy_2O_3	bd	-	bd	-	0.40	0.26	0.58	0.43	0.43	bd	1.18
Y_2O_3	bd	-	bd	-	1.10	0.93	1.81	1.52	0.71	bd	1.99
ThO_2	bd	-	bd	-	1.00	0.43	1.03	0.45	1.05	0.20	2.06
UO_2	1.64	1.18	2.16	0.56	1.86	0.06	1.90	0.28	2.61	1.53	5.50
PbO	bd	-	bd	-	0.94	0.48	0.57	0.45	1.04	0.25	2.52
Nb_2O_5	58.08	2.56	55.06	1.15	54.26	1.13	53.21	0.84	47.56	41.76	54.36
Ta_2O_5	4.38	2.53	2.96	1.08	3.27	0.59	3.75	0.51	4.74	3.24	6.83
SrO	bd	-	bd	-	0.13	0.27	0.29	0.30	0.42	bd	1.40
BaO	bd	-	bd	-	bd	-	0.06	0.15	0.81	bd	2.89
ZrO_2	bd	-	bd	-	0.02	0.05	0.01	0.04	0.37	bd	1.53
F	4.88	0.51	2.98	1.78	4.55	0.53	3.79	1.17	1.85	bd	3.27
Total	98.10		88.51		96.79		92.13		85.05		
O_2=F	2.05		1.25		1.91		1.60		0.78		
Total	96.05		87.25		94.88		90.53		84.27		
ΣREE_2O_3	14.43		14.02		13.28		13.90		9.230		
Na	0.837		0.339		0.897		0.390		0.226		
Ca	0.260		0.201		0.256		0.181		0.088		
K	-		-		-		-		0.035		
LREE	0.342		0.336		0.299		0.307		0.190		
HREE	-		-		0.022		0.028		0.015		
Y	-		-		0.039		0.065		0.023		
Th	-		-		0.015		0.016		0.015		
U	0.024		0.032		0.028		0.028		0.036		
Pb	-		-		0.017		0.010		0.017		
Sr	-		-		0.005		0.011		0.015		
Ba	-		-		-		0.002		0.019		
ΣA	1.463		0.907		1.577		1.038		0.679		
Fe^{3+}	-		-		-		-		0.008		
Al	-		-		-		-		0.017		
Si	-		0.099		-		0.001		0.334		
Ti	0.231		0.213		0.298		0.316		0.237		
Nb	1.591		1.635		1.642		1.613		1.315		
Ta	0.073		0.053		0.059		0.068		0.079		
Zr	-		-		0.001		-		0.011		
ΣB	2.000		2.000		2.000		2.000		2.000		
F	1.005		0.619		0.963		0.804		0.357		
#Nb	90.18	90.97	90.43	91.07	77.26	81.00	85.15		84.61		
#Nb	85.49		86.02		82.13		80.75		80.65		
#Ti	10.64		11.20		14.90		15.83		14.52		

Note: 1 = WDS analyses; 2 = EDS analyses. Other symbols as in Table 1.

Table 3. Chemistry (wt.%) of pyrochlore-group minerals from the Katugin aegirine granites (WDS analyses).

	1							2		
	I		II		III			I	II	III
	n=42	sd	n=46	sd	n=23	min	max	n=8	n=14	n=9
SiO_2	0.04	0.19	0.08	0.27	5.07	1.23	9.05	bd	bd	5.50
TiO_2	7.57	0.87	7.49	0.73	6.47	4.52	10.01	7.76	7.51	5.94
Al_2O_3	bd	-	bd	-	0.18	bd	0.38	bd	bd	0.35
Fe_2O_3	bd	-	bd	-	1.18	bd	2.89	bd	bd	0.05
MnO	bd	-	bd	-	1.24	bd	2.09	bd	bd	bd
CaO	2.68	0.21	2.61	0.20	1.56	bd	2.98	0.69	0.68	0.81
Na_2O	6.67	0.63	2.68	0.55	2.03	0.63	3.96	4.93	2.83	1.47
K_2O	bd	-	bd	-	0.46	bd	1.67	bd	bd	0.72
Ce_2O_3	8.36	0.56	8.26	0.45	4.1	bd	7.67	7.42	7.18	5.60
La_2O_3	2.22	0.67	2.18	0.61	0.68	bd	1.45	1.48	1.44	0.73
Pr_2O_3	0.93	0.08	0.91	0.07	0.45	0.15	0.82	0.82	0.83	0.52
Nd_2O_3	2.89	0.34	2.80	0.28	1.23	0.47	2.14	2.88	2.76	1.42
Sm_2O_3	0.75	0.05	0.74	0.05	0.34	0.12	0.57	1.01	0.99	0.48
Gd_2O_3	0.54	0.05	0.51	0.07	0.26	bd	0.46	1.13	1.08	0.55
Dy_2O_3	0.35	0.04	0.35	0.06	0.21	bd	0.40	1.11	1.05	0.72
Y_2O_3	0.88	0.18	0.82	0.12	0.06	bd	0.50	3.84	3.70	0.96
ThO_2	1.12	0.11	1.13	0.10	1.39	0.80	1.91	0.75	0.70	0.93
UO_2	1.85	0.11	1.84	0.24	2.46	bd	5.62	1.77	1.75	2.78
PbO	0.57	0.10	0.60	0.14	0.98	bd	3.52	0.18	0.23	0.86
Nb_2O_5	54.21	2.76	53.31	2.48	50.66	40.22	63.26	53.22	51.75	47.97
Ta_2O_5	3.08	0.47	2.77	0.05	4.23	bd	10.91	3.53	3.56	4.96
SrO	0.04	0.10	0.05	0.11	0.02	bd	0.17	bd	0.03	0.02
ZrO_2	bd	-	bd	-	bd	bd	bd	bd	bd	0.31
F	4.78	0.54	3.74	1.45	1.00	0.55	3.55	4.94	4.00	1.44
Total	99.54		92.88		85.86			97.45	92.06	85.10
O_2=F	2.01		1.58		0.42			2.08	1.69	0.61
Total	97.53		91.30		84.51			95.37	90.37	84.49
ΣREE_2O_3	16.05		15.75		7.18			15.84	15.33	10.01
Na	0.833		0.339		0.231			0.620	0.365	0.170
Ca	0.185		0.183		0.098			0.048	0.049	0.052
K	-		-		0.034			-	-	0.055
Mn	-		-		0.122			-	-	-
LREE	0.355		0.354		0.143			0.320	0.319	0.190
HREE	0.019		0.018		0.009			0.047	0.046	0.025
Y	0.030		0.028		0.002			0.132	0.131	0.031
Th	0.016		0.017		0.019			0.011	0.011	0.013
U	0.027		0.027		0.032			0.026	0.026	0.037
Pb	0.010		0.011		0.015			0.003	0.004	0.014
Sr	0.002		0.002		0.001			-	0.001	0.001
ΣA	1.477		0.979		0.706			1.207	0.952	0.586
Fe^{3+}	-		-		0.051			-	-	0.002
Al	-		-		0.012			-	-	0.025
Si	0.003		0.005		0.289			-	-	0.329
Ti	0.366		0.369		0.277			0.378	0.376	0.268
Nb	1.577		1.577		1.305			1.560	1.559	1.295
Ta	0.054		0.049		0.066			0.062	0.065	0.082
ΣB	2.000		2.000		2.000			2.000	2.000	2.000
F	0.973		0.774		0.181			1.014	0.844	0.272
#Nb	78.96		79.05		79.05			77.98	77.96	78.86
#Ti	18.34		18.48		18.48			18.90	18.81	16.23
#Ta	2.70		2.47		2.47			3.11	3.23	4.91

Note: 1 = pyrochlore-group minerals from common (1) and ore-rich (2) aegirine granites. Other symbols as in Table 1.

Peer-reviewed version available at *Minerals* **2019**, *9*, 490; doi:10.3390/min9080490

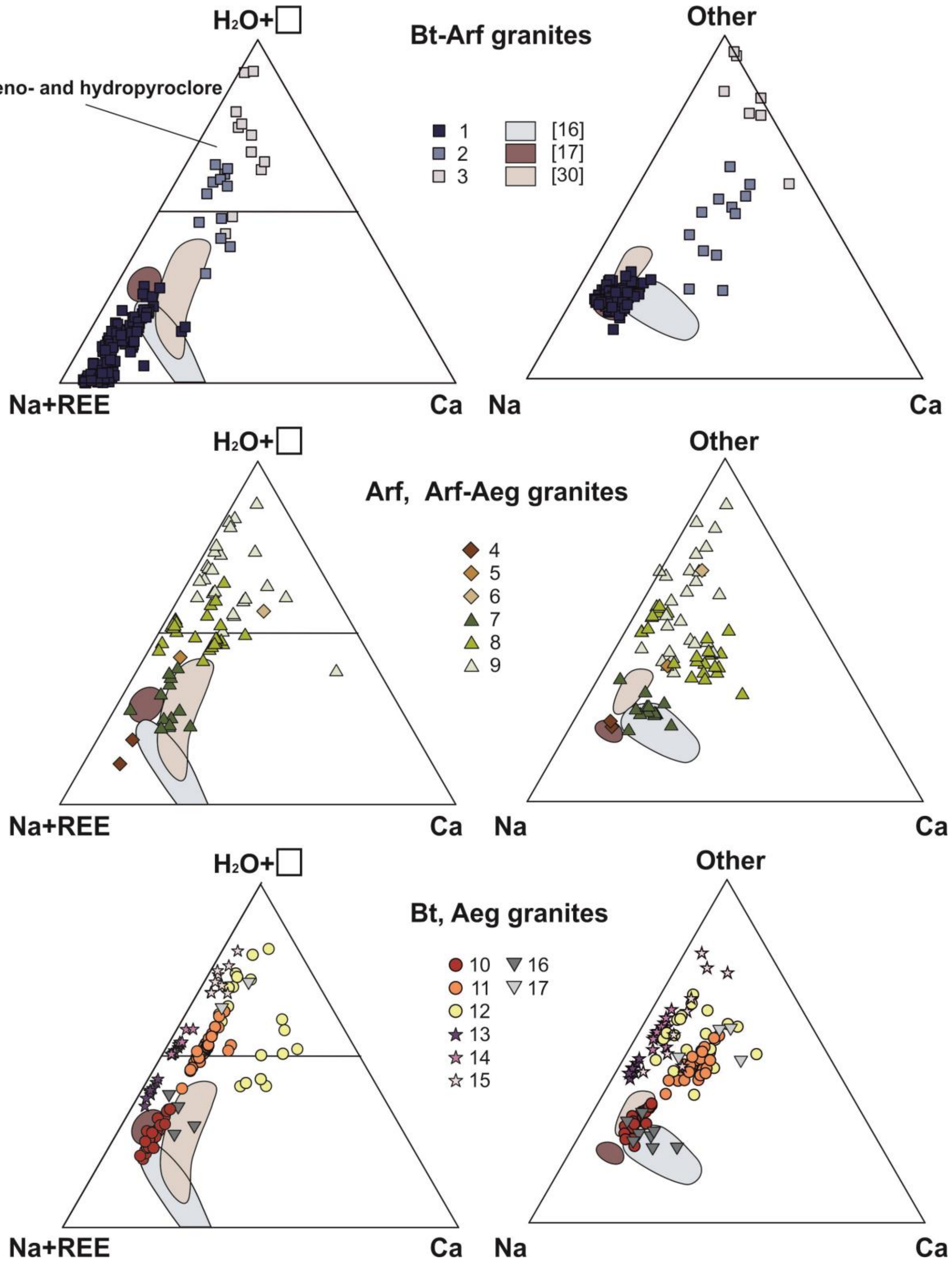

Figure 4. Ternary classification diagrams (A-site) for pyrochlore-group minerals from the Katugin granites. Legend same as in Fig. 3. In the Ca-Na+REE-H_2O+□ diagrams, Ca stands also for other divalent cations (Mn, Pb, Sr, Ba); Na+REE stands also for Y, U, Th, and K.

62 wt.% Nb_2O_5) but has low TiO_2 of 2.4 to 3.8 wt.% (Fig.3). Some pyrochlore grains in these granites are zoned, possibly according to growth (Fig.2 b), with Ta_2O_5-rich (to 15 wt.%) lighter-color zones. Ta enrichment may result from accumulation in evolving granitic melt [7]. The Bt-Arf granite-hosted pyrochlore shows the most complete cation occupancy of the A-site (1.55-2 apfu), with high REE (16.7 wt.% $LREE_2O_3$ and 1.6 wt.% $HREE_2O_3$) and 1.3 wt.% Y_2O_3 but low UO_2 (0.3-0.9 wt.%) and PbO (to 0.21 wt.%). The contents of CaO vary from 1.4 to 3.5 wt.%, with the Na/Ca ratio from 3.7 to 13 (7.1 on average). Fluorine reaches 5.34 wt.% or 1.15 apfu. The LREE/HREE and Y/Ce ratios vary from 8 to

Peer-reviewed version available at *Minerals* **2019**, *9*, 490; doi:10.3390/min9080490

37 and 0.04 to 0.34, with the averages 18.2 and 0.16, respectively. The general formula of this pyrochlore can be expressed as $(Na_{1.2}Ca_{0.18}LREE_{0.36}HREE_{0.04}Y_{0.03}U_{0.02}Th_{0.02})_{1.85}(Nb_{1.8}Ti_{0.15}Ta_{0.05})_2O_{5.94}F_{1.06}$.

First-generation pyrochlores from Bt, Bt-Rbk granites of phase I and Arf, Aeg-Arf and Aeg granites of phase III are compositionally similar (Table 2-3) and differ from that in the ore-rich Aeg granite. Pyrochlore from the ore-rich Aeg granite contains less CaO (0.63-0.85 wt.%) and relatively high $HREE_2O_3$ (2.4 wt.%) and Y_2O_3 (4 wt.%) (Table 3); it has the highest ratios of Na/Ca (10.2-15.2) and Y/Ce (0.72-0.81) but lowest LREE/HREE (6.5-7.7) compared to the counterparts from other granite types (Fig. 5).

The betafite component (#Ti) with 3.75 to 8 wt.% TiO_2 increases progressively from 9.8 % in Bt and Bt-Rbk granites to 19.9 % in Aeg granite while pyrochlore (#Nb) decreases correspondingly (Fig.3); the microlite component (#Ta) varies from 2 to 4.4 wt.% Ta_2O_5. The A occupancy in pyrochlores from Bt, Bt-Rbk, Arf, Aeg-Arf, and Aeg granites varies from 1 to 1.55 apfu while Na does not exceed 0.95 apfu (8.1 wt.% Na_2O) being on average 0.83 apfu (6.5 wt.% Na_2O). CaO in pyrochlores from Bt, Bt-Rbk and Aeg-Arf granites may have a large range, including within the same sample (2 to 5.5 wt.%; Na/Ca = 2-7.2), but is quite stable (2.3-2.8 wt.%; Na/Ca = 3.7-5) in pyrochlore from all aegirine granites (Fig. 5). The latter also has high REE_2O_3: 15-16 wt.% (LREE/HREE = 16-21; Y/Ce – 0.08-0.23) against 10-14.5 wt.% REE_2O_3 (LREE/HREE = 10-19; Y/Ce = 0.1-0.25) in pyrochlores from other granite types. UO_2, ThO_2 and PbO do not exceed 2.6 wt.%, 1.8 wt.%, and 1.4 wt.%, respectively. F is 3.6 to 5.5 wt.% (4.6 wt.% on average).

4.2. Second-generation pyrochlore

Later pyrochlore differs from that of first generation in low contents of Na_2O (1-4.5 wt.%, 2.8 wt.% on average), lower F (2-5 wt.%, 4 wt.% on average), and less occupancy of A- and Y-sites (Tables 1-3; Figs. 4-5). Other cations have concentrations commensurate with those in early pyrochlore.

4.3. Third-generation pyrochlore

The composition of third-generation pyrochlore differs in large ranges of both major and trace elements (Table. 1-3, Fig. 3-5) and analytical totals notably below 100%, as well as in the presence of K_2O (up to 2.3 wt.%), BaO (to 3 wt.%), PbO (to 2.5 wt.%), Fe_2O_3 (to 0.6 wt.%) and significant SiO_2 (to 9.2 wt.%). It also contains more ThO_2 (to 2.1 wt.%) and UO_2 (to 5.6 wt.%) and markedly lower concentrations of REE_2O_3, CaO, Na_2O, Nb_2O_5, Ta_2O_5, and F relative to pyrochlores of earlier generations. Most of these pyrochlore samples fall in the field of hydro- or kenopyrochlore (Fig. 4).

5. Discussion

5.1. Comparison with fluornatropyrochlore from other occurrences

Pyrochlores of different generations from the Katugin granites differ notably in their chemistry and show quite large ranges of some element concentrations. First-generation pyrochlore, with high Na and F concentrations and low Ca, is of special interest and can be classified as fluornatropyrochlore. The latter has been rarely found in natural occurrence and became a registered mineral species in 2013 only [20]. In this respect, it is pertinent to compare the Katugin pyrochlore with its counterparts known from other places.

Fluornatropyrochlore from the Boziguoer rare-metal granites in China (the first finding of this mineral) differs from the samples we analyzed in higher concentrations of PbO (to 16.17 wt.%) and UO_2 (5.8 - 7.5 wt.%) [20,30] and much lower Na_2O (5.5-8.5 wt.%) (Fig. 4-5) at quite high Na/Ca ratios of 4.1-6.6. The F contents in the Boziguoer pyrochlore range within 4.6-7.1 wt.% or 1.25 to 1.63 apfu [30]. The 1.25 to 1.63 apfu exceeding the common value of 1 apfu by a factor of ~1.5 requires additional explanation, as the overestiamtion may lead to notable structure distortion.

Peer-reviewed version available at *Minerals* **2019**, *9*, 490; doi:10.3390/min9080490

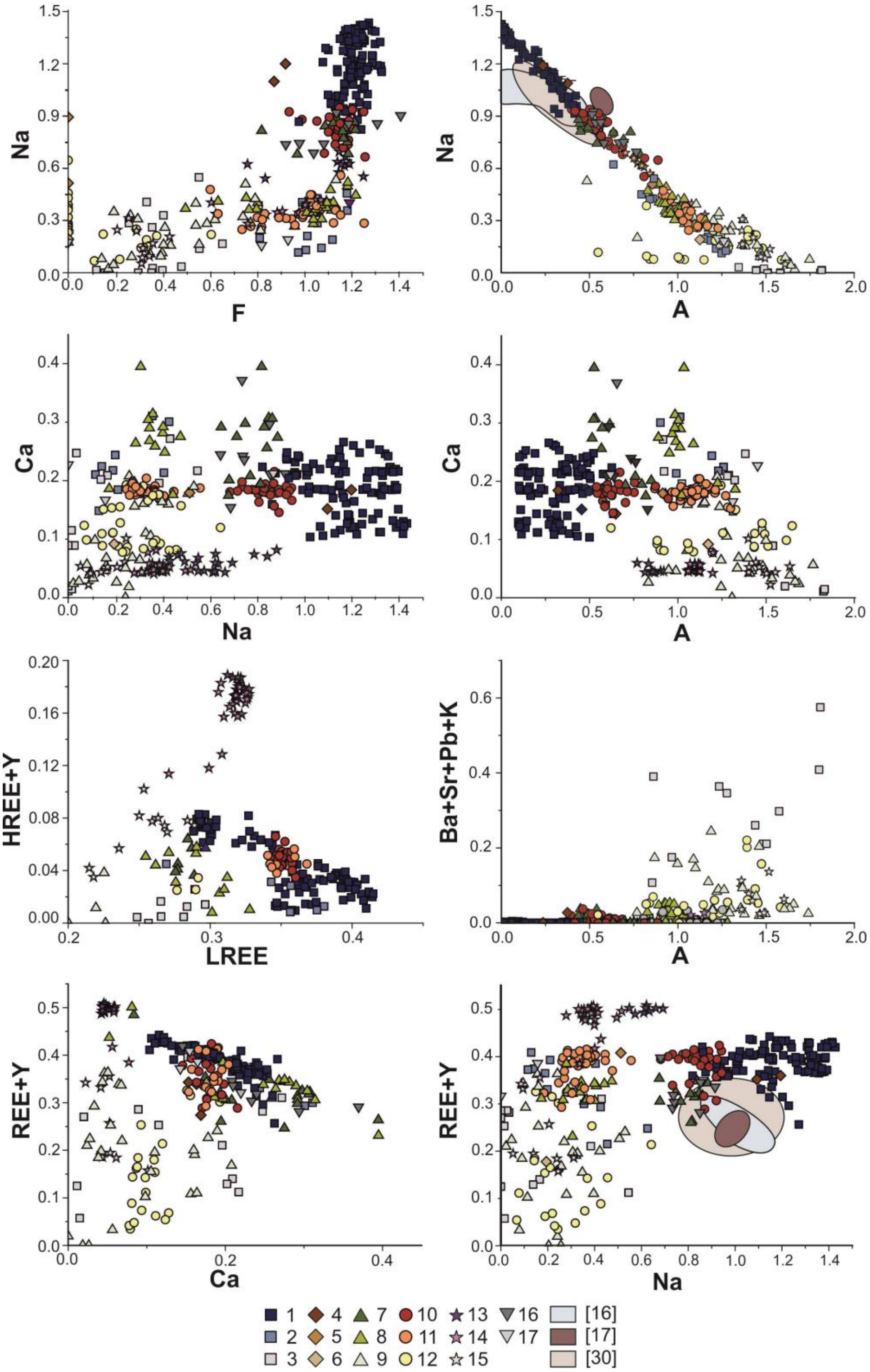

Figure 5. Binary diagrams (apfu) for pyrochlore-group minerals from the Katugin granites. A = vacancy or H_2O at the A-site. The HREE+Y/LREE diagram includes only WDS data. 1-3 = I-, II-, and III-generation pyrochlores from Bt-Arf granite; 4-6 = I-, II-, and III-generation pyrochlores from Arf granite; 7-9 = I-, II-, and III-generation pyrochlores from Arf-Aeg granite; 10-12 = I-, II-, and III-generation pyrochlores from Aeg granite; 13-15 = I-, II-, and III-generation pyrochlores from ore-bearing Aeg granite; 16-17 = I- and II-generation pyrochlores from Bt granite. [16], [17], [30] = fields of fluornatropyrochlores from literature [16,17,30], respectively.

Fluornatropyrochlores with the highest Na contents were reported from the Nechalacho [25,16] and the Mariupol Massif [17] syenites and nepheline syenites but the pyrochlores from both

Peer-reviewed version available at *Minerals* **2019**, *9*, 490; doi:10.3390/min9080490

occurrences have Na_2O lower than in those from the Katugin Bt-Arf granites (7-9.18 wt.% Na_2O against an average of 9.4 wt.%, respectively). On the other hand, they have UO_2 (within 1.1 wt.%), ThO_2 (≤1.6 wt.%) and PbO (≤0.5 wt.%) as low as in the Katugin pyrochlores.

All other published fluornatropyrochlore compositions with high Na/Ca ratios have predominant components with 0.78 to 0.93 #Nb (Fig.3), but their REE_2O_3 contents (mainly LREE) are much lower (to 13.4 wt.%) than in the Katugin pyrochlores (Fig.4). Low Y/Ce ratios (0.12-0.2) in all Katugin pyrochlores we analyzed, except for those from ore-beainrg Aeg granite (Y/Ce to 0.8), are similar to the ratios reported for their counterparts from other occurrences.

5.2. Isomorphism in the Katugin pyrochlores

Judging by their chemistry, pyrochlore-group minerals are prone to extensive iso- and hetero-valent isomorphic substitutions at all sites, which follow hardly decipherable scenarios. Incorporation of HFSE (REE^{3+}, U^{4+} and Th^{4+}) in early pyrochlore likely compensates for Na excess with respect to the ideal neutral formula $NaCaNb_2O_6F$, at complete X occupancy. Therefore, the substitution is expected to proceed as $2Ca^{2+} \rightarrow Na^{+}+REE^{3+}$; $3Ca^{2+} \rightarrow 2Na^{+}+U^{4+}(Th^{4+})$. However, the correlation restricted to Ca vs. REE+Y (r = -0.87 to -0.97) (Fig.5) suggests rather the scenario $3Ca^{2+} \rightarrow 2REE^{3+}$. On the other hand, Na correlates inversely with the A-site vacancy (r = -0.85 to -0.99) (Fig.5), and its poor correlation with F is inconsistent with the $Na^{+}+F^{-} \rightarrow A+Y$ substitution, where A and Y are the respective site vacancies. The Na-A correlation may result from incorporation of the H_3O^{+} group at A as $Na^{+} \rightarrow H_3O^{+}$, or by some more intricate substitution. The correlation of Na and F is better in second-generation pyrochlore ($Na^{+}+F^{-} \rightarrow A+Y$), where H_3O^{+} can also substitute for Na^{+}.

Significant amounts of silica found in third-generation pyrochlore may occur as small inclusions of amorphous SiO_2. However, since high-Si pyrochlores were reported previously [1, etc.], we infer that silica may be isomorphic impurity rather than being SiO_2 mineral inclusions.

5.3. Genesis of different pyrochlore generations in the Katugin rare-metal deposit

It was previously found out that REE phases in the Katugin alkaline granites crystallized after main rock-forming minerals (feldspar and quartz) from residual melt rich in Fe, Na, HFSE, Zn, Sn and volatiles (F, CO_2, P, S, and H_2O) [27]. First-generation pyrochlore is the earliest REE phase. Ultimately high contents of F and Na indicate their high activity during crystallization of pyrochlore which was synchronous with or slightly postdating the formation of melanocratic phases (aegirine, biotite, and arfvedsonite). Fe extracted from the melt became bound in the melanocratic minerals, which hindered the crystallization of columbite [2].

Second-generation pyrochlore likely formed at the early postmagmatic stage in the evolution of the Katugin complex, judging by the presence of generation I and II pyrochlores enclosed in zircon which was previously interpreted as magmatic or early postmagmatic [23,31].

Third-generation pyrochlore may have replaced the earlier phases during supergene alteration processes after the formation of the Katugin ore deposit, whereby pyrochlore gained K, Fe, Mn, Si, Th, and U but lost REE, Ca, Na, Nb, and Ta.

The compositional variations of pyrochlore-group minerals in granitic systems remain poorly investigated because of their rare occurrence. Minerals of this group were studied in carbonatites, where many authors [1,5,32,33] distinguished similar formation and transformation stages in the course of magmatic, postmagmatic, and supergene evolution.

Although being different in high Ca contents (about 1 apfu in magmatic pyrochlore), carbonatite-hosted pyrochlores show composition trends similar to those revealed in their Katugin granite-hosted analogs: progressive decrease in Na and F from magmatic to postmagmatic varieties, at invariable Ca and slightly variable relative amounts of cations at the B-site. The Katugin late pyrochlore shares chemical similarity with the pyrochlore variety classified as supergene [33].

6. Conclusions

1. The Katugin granites store pyrochlore of three generations which formed, respectively, during late magmatic and early postmagmatic evolution of the complex and later supergene alteration.

2. Primary magmatic pyrochlore is fluornatropyrochlore with high Na/Ca ratios, which is of extremely rare natural occurrence (only few sites in the world are known). Some pyrochlore samples from the Katugin deposit contain as much as 10.7 wt.% Na_2O exceeding all previously reported values.
3. Early postmagmatic pyrochlore has lower concentrations of Na and F than the primary phase, while the contents of other elements are commensurate.
4. Supergene postmagmatic pyrochlore differs in markedly lower REE, Ca, Nb, and Ta and zero Na and F, as well as in the presence of Si, K, Ba, Pb and Fe.
5. The Katugin pyrochlores contain more REE_2O_3 than their high-Na counterparts from other known occurrences, but the Y/Ce ratios are as low as elsewhere. They are compositionally similar especially to fluornatropyrochlore hosted by syenite and nepheline syenite at the deposits of Nechalacho (Canada) and Mariupol Massif (Ukraine).

Author Contributions: Conceptualization, A.E.S. and E.P.B.; formal analysis, A.E.S., E.A.K. and S.V.K.; investigation, A.E.S., E.P.B.; resources, A.E.S., E.P.B. and E.V.S.; writing—original draft preparation, A.E.S. and E.P.B; writing—review and editing, A.E.S., E.V.S. and V.B.S; visualization, A.E.S.

Funding: This research was funded by the Russian Foundation for Basic Research (Project 16-35-60054 mol_a_dk). Scanning Electron Microscopy was funded by the Russian Science Foundation (Project 14-17-00325). WDS was carried out as part of government assignment to the V.S. Sobolev Institute of Geology and Mineralogy.

Acknowledgments: We thank T. Perepelova and V.V. Sharygin for assistance in manuscript preparation.

Conflicts of Interest: Authors declare no conflicts of interest.

References

1. Nasraoui, M.; Bilal, E. Pyrochlores from the Lueshe carbonatite complex (Democratic Republic of Congo): a geochemical record of different alteration stages. *Journal of Asian Earth Sciences*, **2000**, *Volume 18*, pp. 237-251. https://doi.org/10.1016/S1367-9120(99)00056-5
2. Ogunleye, P.O.; Garba, I.; Ike, E.C. Factors contributing to enrichment and crystallization of niobium in pyrochlore in the Kaffo albite arfvedsonite granite, Ririwai Complex, Younger Granites province of Nigeria. *Journal of African Earth Sciences*, **2006**, *Volume 44*, pp. 372-382. https://doi.org/10.1016/j.jafrearsci.2005.12.006
3. Yaroshevskii, A.A.; Bagdasarov, Yu.A. Geochemical diversity of minerals of the pyrochlore group. *Geochemistry International*, **2008**, *Volume 46 (12)*, pp. 1245-1266. https://doi.org/10.1134/S0016702908120045
4. Cordeiro, P.F.O.; Brod, J.A.; Palmierie, M.; Oliveria, C.G.; Barbosa, E.S.R.; Santos, R.V.; Gaspar, J.C.; Assis, L.C. The Catalao I niobium deposit, central Brazil: resources, geology and pyrochlore chemistry. *Ore Geology Review*, **2011**, *Volume 41*, pp. 112–121. https://doi.org/10.1016/j.oregeorev.2011.06.013
5. Mitchell, R.H. Primary and secondary niobium mineral deposits associated with carbonatites. *Ore Geology Reviews*, **2015**, *Volume* 64, pp. 626-641. https://doi.org/10.1016/j.oregeorev.2014.03.010
6. Khromova, E.A.; Doroshkevich, A.G.; Sharygin, V.V.; Izbrodin, L. A. Compositional evolution of pyrochlore-group minerals in carbonatites of the Belaya Zima Pluton, Eastern Sayan. *Geology of Ore Deposits*, **2017**, *Volume 59*, pp. 752-764. https://doi.org/10.1134/S1075701517080037
7. Hogarth, D.D. Classification and nomenclature of the pyrochlore group. *American Mineralogist*, **1977**, *Volume 62*, pp. 403-410.
8. Atencio, D.; Andrade, M.B.; Christy, A.G.; Gieré, R.; Kartashov, P.M. The pyrochlore supergroup of minerals: nomenclature. *Canadian Mineralogist*, **2010**, *Volume 48*, pp. 673-698. https://doi.org/10.3749/canmin.48.3.673
9. Christy, A.G.; Atencio, D. Clarification of status of species in the pyrochlore supergroup. *Mineralogical Magazine*, **2013**, *Volume 77(1)*, pp. 13-20. https://doi.org/10.1180/minmag.2013.077.1.02
10. Guowu, L.; Guangming, Y.; Fude, L.; Ming, X.; Baoming, P.; de Fourestier, J. Fluorcalciopyrochlore, a new mineral species from Bayan Obo, Inner Mongolia, P.R. China. *Canadian Mineralogist*, **2016**, *Volume 54*, pp. 1285-1291. https://doi.org/10.3749/canmin.1500042

11. Donskaya, T.V.; Gladkochub, D.P.; Sklyarov, E.V.; Kotov, A.B.; Larin, A.M.; Starikova, A.E.; Mazukabzov, A.M.; Tolmacheva, E.V.; Velikoslavinski, S.D. Genesis of the Paleoproterozoic rare-metal granites of the Katugin Massif. *Petrology*, **2018**, *Volume 26 (1)*, pp. 47–64. https://doi.org/10.1134/S0869591118010022
12. Podkovyrov, V.N.; Kotov, A.B.; Larin, A.M.; Kotova, L.N.; Kovach, V.P.; Zagornaya, N.Yu. Sources and provenances of lower Proterozoic terrigenous rocks of the Udokan Group, Southern Kodar-Udokan depression: Results of Sm-Nd isotopic investigations. *Doklady Earth Sciences*, **2006**, *Volume 408 (4)*, pp. 518-522. https://doi.org/10.1134/S1028334X06040027
13. Gladkochub, D.P.; Donskaya, T.V.; Sklyarov, E.V.; Kotov, A.B.; Vladykin, N.V.; Pisarevsky, S.A.; Larin, A.M.; Salnikova, E.B.; Saveleva, V.B.; Sharygin, V.V.; Starikova, A.E.; Tolmacheva, E.V.; Velikoslavinsky, S.D.; Mazukabzov, A.M.; Bazarova, E.P.; Kovach, V.P.; Zagornaya, N.Yu.; Alymova, N.V.; Khromova, E.A. The unique Katugin rare-metal deposit (southern Siberia): Constraints on age and genesis. *Ore Geology Reviews*, **2017**, *Volume 91*, pp. 246-263. https://doi.org/10.1016/j.oregeorev.2017.10.002
14. Prokhorov, K.V.; Sobachenko, V.N. Structural-petrological and geochemical conditions of the formation of ore-bearing high-temperature sodic metasomatites. In: *Structure of Ore-Bearing Precambrian Faults*. Moscow: Nauka, Russia, 1985, pp. 94-121. (in Russian)
15. Timofeev, A.; Williams-Jones, A.E. The origin of niobium and tantalum mineralization in the Nechalacho REE Deposit, NWT, Canada. *Economic Geolog*, **2015**, *Volume 110*, pp. 1719–1735. https://doi.org/10.2113/econgeo.110.7.1719
16. Moller, V.; Williams-Jones, A.E. Petrogenesis of the Nechalacho layered suite, Canada: Magmatic evolution of a REE–Nb-rich nepheline syenite intrusion. *Journal of Petrology*, **2016**, *Volume* 57(2), pp. 229–276. https://doi.org/10.1093/petrology/egw003
17. Dumanska-Slowik, M.; Pieczka, A.; Tempesta, G.; Olejniczak, Z.; Heflik, W. "Silicified" pyrochlore from nepheline syenite (mariupolite) of the Mariupol Massif, SE Ukraine: A new insight into the role of silicon in the pyrochlore structure. *American Mineralogist*, **2014**, *Volume 99*, pp. 2008–2017. https://doi.org/10.2138/am-2014-4896
18. Siegel, K.; Vasyukova, O.V.; Williams-Jones, A.E. Magmatic evolution and controls on rare metal-enrichment of the Strange Lake A-type peralkaline granitic pluton, Québec-Labrador. *Lithos*, **2018**, *Volume 308–309*, pp. 34–52. https://doi.org/10.1016/j.lithos.2018.03.003
19. Kovalenko ,V.I.; Yarmolyuk, V.V.; Kartashov, P.M.; Kozlovskii, A.M.; Listratova, E.N.; Salnikova, E.B.; Kovach, V.P.; Kozakov, I.K.; Kotov, A.B.; Yakovleva, S.Z.; Ponomarchuk, V.A. The Khaldzan-Buregtei massif of peralkaline rare-metal igneous rocks: Structure, geochronology, and geodynamic setting in the caledonides of Western Mongolia. *Petrology*, **2004**, *Volume 12(5)*, pp. 412-436.
20. Yin, J.; Li, G.; Yang, G.; Ge, X.; Xu, H.; Wang, J. Fluornatropyrochlore, a new pyrochlore supergroup mineral from the Boziguoer rare earth element deposit, Baicheng County, Akesu, Xinjiang, China. *Canadian Mineralogist*, **2015**, *Volume 53(3)*, pp. 455-460. https://doi.org/10.3749/canmin.1500007
21. Archangelskaya, V.V.; Ryabtsev, V.V.; Shuriga, T.N. Geological structure and mineralogy of the tantalum deposits of Russia. In *Mineral commodities*; Moscow: VIMS, Russia, 2012; Volume 26, 318 p. (in Russian)
22. Sklyarov, E.V.; Gladkochub, D.P.; Kotov, A.B.; Starikova, A.E.; Sharygin, V.V.; Velikoslavinsky, S.D.; Larin, A.M.; Mazukabzov, A.M.; Tolmacheva, E.A.; Khromova, E.A. Genesis of the Katugin rare-metal ore deposit: magmatism versus metasomatism. *Russian Journal of Pacific Geology*, **2016**, *Volume 35 (3)*, pp. 9-22. https://doi.org/10.1134/S1819714016030064
23. Kotov, A.B.; Vladykin, N.V.; Larin, A.M.; Gladkochub, D.P.; Salnikova, E.V.; Sklyarov, E.V.; Tolmacheva, E.V.; Donskaya, T.V.; Velikoslavinsky, S.D.; Yakovleva, S.Z. New data on the age of ore formation in the unique Katugin rare-metal deposit (Aldan Shield). *Doklady Earth Sciences*, **2015**, *Volume 463 (1)*, pp. 663-667. https://doi.org/10.1134/S1028334X15070107
24. Bykov, Yu.V.; Archangelskaya, V.V. Katugin rare-metal deposit. In *Transbaikalian Deposits*. Moscow: Geoinformmark, Russia, 1995, Volume 1 (5), pp. 76-85. (in Russian)
25. Archangelskaya, V.V.; Kazanskii, V.I.; Prokhorov, K.V.; Sobachenko, V.N. Geological structure, zoning and conditions of formation of the Katugin Ta-Nb-Zr deposit (Chara-Udokan district, East Siberia). *Geology of Ore Deposits*, **1993**, *Volume 35 (2)*, pp. 115-131.
26. Ryabtsev, V.V.; Chistov, I.V.; Shuriga, T.N. Tantalum ores of Russia: state and prospects of the development of the raw mineral base. In *Mineral commodities*; Moscow: VIMS, Russia, 2006; Volume 21, 92 p. (in Russian)

Peer-reviewed version available at *Minerals* **2019**, *9*, 490; doi:10.3390/min9080490

27. Savelieva, V.B.; Bazarova, E.P.; Khromova, E.A.; Kanakin, S.V. Rare-earth minerals in rocks of the Katugin rare-metal deposit (East Transbaikalia): behavior of lanthanides and Y during crystallization of the saturated-in-fluorine agpaitic melt. *Zapiski RMO* (Transactions of RMS), **2017**, *Volume 146 (4)*, pp. 1-21. (in Russian)
28. Savelieva, V.B.; Bazarova, E.P.; Khromova, E.A.; Kanakin, S.V. Fluorides and fluorcarbonates in rocks of the Katugin complex, Eastern Siberia: indicators of geochemical mineral formation conditions. *Geology of Ore Deposits*, **2017**, *Volume 59 (7)*, pp. 561-574. https://doi.org/10.1134/S1075701517070108
29. Larin, A.M.; Kotov, A.B.; Vladykin, N.V.; Gladkochub, D.P.; Kovach, V.P.; Sklyarov, E.V.; Donskaya, T.V.; Velikoslavinskii, S.D.; Zagornaya, N.Yu.; Sotnikova I.A. Rare metal granites of the Katugin complex (Aldan Shield): Sources and geodynamic formation settings. *Doklady Earth Sciences*, **2015**, *Volume 464 (1)*, pp. 889-893. https://doi.org/10.1134/S1028334X15090056
30. Huang, H.; Wang, T.; Zhang, Zh.; Li, Ch.; Qin, Q. Highly differentiated fluorine-rich, alkaline granitic magma linked to rare metal mineralization: A case study from the Boziguo'er rare metal granitic pluton in South Tianshan Terrane, Xinjiang, NW China. *Ore Geology Reviews*, **2018**, *Volume 96*, pp. 146–163. https://doi.org/10.1016/j.oregeorev.2018.04.021
31. Levashova, E.V.; Skublov, S.G.; Marin, Y.B.; Lupashko, T.N.; Ilchenko, E.A. Trace elements in zircon from rocks of the Katugin rare-metal deposit. *Geology of Ore Deposits*, **2015**, *Volume 57 (7)*, pp. 579-590. https://doi.org/10.1134/S1075701515070077
32. Lumpkin, G.R.; Ewing, R.C. Geochemical alteration of pyrochlore group minerals: Pyrochlore subgroup. *American Mineralogist*, **1995**, *Volume 80*, pp. 732-743. https://doi.org/10.2138/am-1995-7-810
33. Torro, L.; Villanova, C; Castillo, M; Goncalves, A.O.; Melgarejo, J.C. Niobium and rare earth minerals from the Virulundo carbonatite, Namibe, Angola. *Mineralogical Magazine*, **2012**, *Volume* 76(2), pp. 393–409. https://doi.org/10.1180/minmag.2012.076.2.08